International Journal of Pharmaceutics 400 (2010) 211–220

Contents lists available at ScienceDirect

International Journal of Pharmaceutics

journal homepage: www.elsevier.com/locate/ijpharm

Pharmaceutical Nanotechnology

Synthesis and *in vitro*/*in vivo* anti-cancer evaluation of curcumin-loaded chitosan/poly(butyl cyanoacrylate) nanoparticles

Jinghua Duan[a,1], Yangde Zhang[a,1], Shiwei Han[a], Yuxiang Chen[a], Bo Li[b], Mingmei Liao[a], Wei Chen[a], Xingming Deng[c], Jinfeng Zhao[a,*], Boyun Huang[d]

[a] *Key Laboratory of Nanobiological Technology, Ministry of Health National Hepatobiliary and Enteric Surgery Research Center, Central South University, Changsha, Hunan 410008, PR China*
[b] *Department of Pathology, Xiangya School of Medicine, Central South University, Changsha, Hunan 410008, PR China*
[c] *Division of Cancer Biology and Department of Radiation Oncology, Emory University School of Medicine, Atlanta, GA 30322 USA*
[d] *State Key Laboratory for Power Metallurgy, Central South University, Changsha, Hunan 410008, PR China*

ARTICLE INFO

Article history:
Received 10 May 2010
Received in revised form 24 July 2010
Accepted 25 August 2010
Available online 8 September 2010

Keywords:
Curcumin
Chitosan-coated poly(butyl) cyanoacrylate nanoparticles
Hepatocellular carcinoma cells
Hepatocarcinoma tumor xenografts

ABSTRACT

We have synthesized novel cationic poly(butyl) cyanoacrylate (PBCA) nanoparticles coated with chitosan, formulation of curcumin nanoparticles. The size and zeta potential of prepared curcumin nanoparticles were about 200 nm and +29.11 mV, respectively with 90.04% encapsulation efficiency. The transmission electron microscopy (TEM) study revealed the spherical nature of the prepared nanoparticles along with confirmation of particle size. Curcumin nanoparticles demonstrate comparable *in vitro* therapeutic efficacy to free curcumin against a panel of human hepatocellular cancer cell lines, as assessed by cell viability (3-[4,5-dimethylthiazol-2-yl]2,5-diphenyltetrazolium bromide assay [MTT assay]) and proapoptotic effects (annexin V/propidium iodide staining). *In vivo*, curcumin nanoparticles suppressed hepatocellular carcinoma growth in murine xenograft models and inhibited tumor angiogenesis. The curcumin nanoparticles' mechanism of action on hepatocellular cancinoma cells is a mirror that of free curcumin.

1. Introduction

Curcumin, a yellow polyphenol extracted from the rhizome of turmeric (*Curcuma longa*), is been extensively used in China, India and southeast tropical Asia as a spice and colouring material, and a treatment for a wide variety of ailments including biliary disorders, hepatic disorders, diabetic wounds, anorexia, rheumatism, and sinusitis (Goel et al., 2008; Aggarwal and Harikumar, 2009; Anand et al., 2007). Recent studies have shown that curcumin, either alone or in combination with other anticancer agents, has potent anticancer effects. This was evidenced by its inhibitory effects on the growth of a number of tumor cell lines *in vitro* and *in vivo*, including melanoma, mantle cell lymphoma (MCL), hepatic, prostatic, ovarian, and pancreatic carcinomas (Aggarwal et al., 2003; Siwak et al., 2005; Gururaj et al., 2002; Belakavadi and Salimath, 2005; Shishodia et al., 2005; Zheng et al., 2004). Curcumin has been reported to have diverse effects on signaling molecules, such as downregulation of the expression of angiogenesis-associated genes, activation of the apoptotic mechanisms, and induction of the cell cycle arrest (Gururaj et al., 2002; Belakavadi and Salimath, 2005; Shishodia et al., 2005).

Despite great therapeutic potential for curcumin utilization in a variety of diseases, its clinical development has been hindered due to its fast metabolism and poor water solubility (Wang et al., 1997; Tonnesen et al., 2002; Cheng et al., 2001; Shoba et al., 1998). The main shortcomings of curcumin are its lipophilicity hence, low bioavailability, degradation at alkaline pH and photodegradation. Lipophilic nature of curcumin makes it vulnerable to RES uptake and hence it can't reach the therapeutic target with therapeutic concentration.

To increase its aqueous solubility and bioavailability, attempts have been made through encapsulation in liposome, polymeric nanoparticle, lipid-based nanoparticle, biodegradable microsphere, cyclodextrin and hydrogel (Bisht et al., 2007; Tiyaboonchai et al., 2007; Kunwar et al., 2006; Sou et al., 2008; Salmaso et al., 2007; Vemula et al., 2006). Interest in nanocarriers for cancer chemotherapy is growing. Nanoparticle-based drug delivery approaches have the potential for rendering hydrophobic agents like curcumin dispersible in aqueous media, thus circumventing the pitfalls of poor solubility.

Design and development of biodegradable controlled drug delivery of therapeutic entities with improved bioavailability is the main research aspect on which extensive work is been done

* Corresponding author. Tel.: +86 731 84327971; fax: +86 731 84327987.
E-mail address: zhaojinfeng@hotmail.com (J. Zhao).
[1] These authors contributed equally to this work.

0378-5173/$ – see front matter © 2010 Elsevier B.V. All rights reserved.
doi:10.1016/j.ijpharm.2010.08.033

in the past few decades. One of the promising and exciting drug delivery system which can meet the above mentioned requirements is polymeric nanoparticles. Among the various promising polymers like PLA, PLGA, polycaprolactone, polymethylidene malonate, poly(butyl) cyanoacrylate (PBCA) nanoparticles meet ideal requirements for controlled drug delivery and passive targeting such as biodegradability, low toxicity, ability to alter the biodistribution of drugs and easy to synthesize and purify (Behan et al., 2001; Juan et al., 2006; Maksimenko et al., 2008; Reddy et al., 2004).

PBCA nanoparticles have been proved to be an effective drug delivery system for the controlled drug delivery of various pharmacologically active moieties, like anticancer agents, analgesics, antibiotics and peptide (Huang et al., 2007; Miyazaki et al., 2003; Page-Clisson et al., 1998; Tasset et al., 1995). The PBCA nanoparticles are generally prepared by emulsion or dispersion polymerization in an acidic aqueous solutions of surfactants forming a porous structure with high specific area on which various quantities of drugs, dissolved in the medium during or after polymerization, can be loaded (Petri et al., 2007). Surface characteristics like zeta potential and the solubility property can be modulated to meet the prerequisites of intravenous administration.

Curcumin has been conjugated with numerous carriers including phospholipids (Maiti et al., 2007), cyclodextrin (Salmaso et al., 2007), phosphatidyl choline (Marczylo et al., 2007), and liposomes (Kunwar et al., 2006), but very little information is available about its biological activities.

In this study, we describe a simple method of synthesis and characterization of a novel cationic poly(butyl) cyanoacrylate nanoparticles coated with chitosan encapsulated formulation of curcumin that can improve the solubility of curcumin and prevents RES uptake. In various kinds of poly(alkyl) cyanoacrylates (PACAs), PBCA was the most used drug carrier because it can interact with different kind of drugs which will aid in increased curcumin entrapment efficiency. The development of a delivery system that can enable parenteral administration of curcumin in an aqueous phase medium will significantly harness the potential of this promising anti-cancer agent in the clinical arena. We investigated the *in vitro* and *in vivo* antitumor activity of curcumin-PBCA nanoparticles against human hepatocellular carcinoma cells. *In vivo*, curcumin nanoparticles inhibited hepatic carcinoma growth and demonstrated antiangiogenic effects.

2. Materials and methods

2.1. Materials

Antibodies used for immunoblotting included polyclonal β-actin antibody (Abgent, USA), anti-cyclooxygenase-2 (COX-2) rabbit polyclonal antibody and anti-vascular endothelial growth factor (VEGF) rabbit polyclonal antibody, which were obtained from Boster Biological Technology, Ltd., Wuhan, China. Donkey anti-rabbit IgG-HRP was purchased from Santa Cruze Biotechnology, USA. The Bicinchoninic acid protein assay kit was from Beyotime Institute of Biotechnology, China and the enhanced chemiluminescence kit was from Pierce, USA. 3-[4,5-Dimethylthiazol-2-yl] 2,5-diphenyltetrazolium bromide (MTT reagent) was purchased from Trevigen, Inc., USA. Annexin V/PI apoptosis detection kit was from Jingmei Biotech Co., Ltd., Beijing, China. Dulbecco's modification of eagle's medium (DMEM) was obtained from Beijing Solarbio Science & Technology Co., Ltd., China. UltraSensitive™ S-P detection kit of immunohistochemistry was purchased from Maixin_Bio Co., Ltd., Fuzhou, China.

Chitosan (degree of deacetylation ≥85%) was purchased from Sigma corporation. Butyl cyanoacrylate (BCA) monomer was synthesized by Guangzhou Baiyun Medical Adhensive Co., Ltd., China. Curcumin was obtained from Sinopharm Chemical Reagent Co., Ltd., China.

Gradient grade methanol were purchased from Merck (Germany) and used as received. All other chemicals used were of analytical reagent grade and without further purification. Ultrapure water was used for the preparation of all solutions.

2.2. Cell lines

The human hepatocellular carcinoma cell lines HepG2, Huh7 and Bel7402 cell lines were provided by ourselves. All kinds of cells were cultured in DMEM with 10% fetal bovine serum (FBS) and 100 U/mL penicillin–streptomycin.

2.3. Preparation of curcumin-PBCA nanoparticles

PBCA nanoparticles were prepared by emulsion polymerization as described in detail elsewhere (Allemann et al., 1993; Couvreur and Vauthier, 1991; Douglas et al., 1984; Lescure et al., 1992; Douglas et al., 1985; Huang et al., 2007). Briefly, chitosan (0.1%, w/v) was dissolved in the polymerization medium containing HCl. Curcumin powder (0.01%, w/v) was then added by first dissolving it separately in a small quantity of ethanol. Finally, the desired amount (100 μL) of BCA monomer was dropped into the acidic solution at room temperature under continuous magnetic stirring, stirring was maintained for at least 6 h until the polymerization was complete. The colloidal suspension obtained was brought to pH value of 6.0 ± 0.5 by adding 0.5 mol/L NaOH to end the polymerization. The nanoparticles were separated by ultracentrifugation at 16,000 rpm (Sigma 3K-18 refrigerated centrifuge, Germany) for 60 min and washed with distilled water at least three times.

Because the temperature and stirring speed have little effect on the formation of poly(butyl)cyanoacrylate (Dai et al., 2004), we use 3^2 factorial design to investigate the parameters like the amount of stabilizer and monomer on zeta potential and percentage of drug entrapment of PBCA nanoparticles. Amount of curcumin was kept constant. The design of all the nine batches taken using 3^2 factorial level is shown in Table 1.

2.4. Characterization of curcumin-PBCA nanoparticles

2.4.1. Particle size and zeta potential

PBCA nanoparticle suspensions were diluted with deionized water to ensure that the signal intensity is suitable for the instrument. Values are presented as mean ± SD from three replicate samples.

Dynamic light scattering measurements for determining the average size and size distribution of the curcumin-PBCA nanoparticles were performed using a Zetasizer $1000HS_A$ (Malvern Instruments Ltd., Worcestershire, UK). The colloidal suspension of the nanoparticles was diluted with deionized distilled water, and the intensity of scattered light was detected at a scattering angle of 90° to an incident beam at a temperature of 25 °C.

Table 1
Experimental study design using 3^2 factorial methods.

Batch	Volume of BCA monomer (μL)	Amount of chitosan (mg)
Nanocurcumin 1	50	5
Nanocurcumin 2	50	10
Nanocurcumin 3	50	20
Nanocurcumin 4	100	5
Nanocurcumin 5	100	10
Nanocurcumin 6	100	20
Nanocurcumin 7	200	5
Nanocurcumin 8	200	10
Nanocurcumin 9	200	20

The zeta potential was measured on Zetasizer Nano system (Malvern Instruments Ltd., Worcestershire, UK). The measurement was done in ultrapure distilled water using disposable zeta cells using the general purpose protocol at 25 °C. The instrument was calibrated routinely with a −50 mV latex standard. The mean zeta potential was determined using phase analysis light scattering technique.

2.4.2. Transmission electron microscopy observation

The surface appearance and shape of curcumin-PBCA nanoparticles was observed by transmission electron microscopy (TEM) using a JEOL-1230 at 100 kV. 1 mL dispersion was diluted with 1 mL demineralized water and a drop of it was placed onto a collodion support on copper grids (200 mesh). About 2 min of deposition, the grid was tapped with a filter paper to remove surface water and negatively stained by using a sodium phosphotungstate for 2 min. After 1 min excess fluid was removed and the grid surface was air dried at room temperature before loaded in the microscope.

2.5. Encapulation of curcumin in PBCA nanoparticles

HPLC system (P680 series, DIONEX, USA) was used for the analysis of the amount of curcumin incorporated in the nanoparticles, with column Hypersil BDS C18 (4.6 × 250 mm, 5 μm) and the mobile phase consisted of methanol and 5% (w/v) of acetic acid at the volume ratio of 70:30. The flow rate was set at 1.0 mL/min and the analysis wavelength was at 420 nm.

The encapsulation efficiency of the drug was calculated as the mass ratio of the amount of the drug entrapped in nanoparticles to that used in the nanoparticle preparation.

The PBCA nanoparticles loaded curcumin was characterized by fluorescence spectra.

2.6. Cell culture assay

2.6.1. In vitro cell viability assays in hepatic cancer cells lines

The cytotoxicity of the free and encapsulated curcumin was determined in HepG2, Huh7 and Bel7402 cell lines using MTT dye assay. Control experiments were carried out using the complete growth culture medium only (serving as non-toxic control). Three kinds of cells (100 μL) at a density of 6×10^4 cells/well were seeded into a 96-well plate in the complete growth culture medium. After culturing for 12 h, the medium was exchanged with 200 μL medium containing a series of different concentration of free curcumin, curcumin-PBCA nanoparticles and empty PBCA nanoparticles (5, 10, 20, 30, 40, 50 μg/mL). After a specified period of time, the culture medium from each well was removed and the cells were washed twice with 1 × PBS. About 200 μL of the complete growth culture medium and 20 μL MTT solution (5 mg/mL in PBS, pH 7.4) were then added to each well. After 4 h of incubation at 37 °C and 5% CO_2, the media were removed and the formazan crystals were solubilized with 150 μL DMSO for 10 min. The amount of formazan was then determined from the optical density at 570 nm by a microscan spectrum (Electro Thermo, Milford, MA, USA). The results were expressed as percentages relative to the result obtained with the non-toxic control.

2.6.2. Curcumin-PBCA nanoparticles uptake in HepG2 cells by fluorescence method

Curcumin is naturally fluorescent in the visible green spectrum. To visualize the cellular uptake of curcumin-PBCA nanoparticles. HepG2 cells were plated in 6 well plate up to 80% confluency. Cells were treated with 30 μg/mL free and curcumin-PBCA nanoparticles. As curcumin is insoluble in aqueous solution, the free curcumin was dissolved with the aid of dimethylsulfoxide (DMSO). The final concentration of DMSO in the culture medium was always <0.1%. After culturing in a 5% CO_2 incubator for prescribed time periods, the cells were washed with 1× PBS three times to remove the nanoparticles in the medium. Cells were examined under a Leica DM LB2 fluorescent microscope (Leica Microsystems Wetzlar GmbH, Germany) for intracellular curcumin fluorescence.

2.6.3. Annexin V/Propidium Iodide staining for apoptotic cells

To determine the effects of curcumin-PBCA nanoparticles on apoptosis, HepG2 cells were stained with annexin V and propidium iodide for fluorescence activated cell sorting (FACS) analysis. Cells were seeded at $2.5–5.0 \times 10^5$ cells per 60 mm plate and incubated until 80% confluency. Cells were treated with various concentrations of curcumin-PBCA nanoparticles. As controls, cells were also incubated with complete growth culture medium only. After 24 h incubation, cells were harvested by quick trypsinization to minimize potentially high annexin V background levels in adherent cells, washed twice with cold PBS, and stained with annexin V-fluorescein 5(6)-isothiocyanate (FITC) and propidium iodide (PI) in binding buffer. Stained cells were placed on ice and protected from light until read via flow cytometry. Processed single cell suspensions were analyzed on a FACS Calibur flow cytometer (BD, Franklin Lakes, NJ, USA) with the laser excitation wavelength set at 488 nm. The green signal from FITC/annexin V was measured at 525 nm and the red signal from PI was measured at 620 nm. Cells staining negative for both annexin V and PI are viable. Cells that are annexin V^+/PI^- are in early apoptosis, whereas cells that are necrotic or in late apoptosis are annexin V^+/PI^+.

2.7. In vivo studies with curcumin-PBCA nanoparticles

2.7.1. Studies on pharmacokinetics in mice

Sprague–Dawley male rats with body weights ranging from 250 to 300 g were used to study the pharmacokinetics of free curcumin and curcumin-PBCA nanoparticles. All animal experiments complied with the requirements of the National Act on the use of experimental animals (People's Republic of China). Curcumin and its nanoparticles formulation were injected intravenously to the rat at doses of 10 and 5 mg/kg, respectively. Each formulation was tested on three rats. After dosing, serial blood samples (0.1–0.2 mL) were obtained at predetermined time intervals after drug administration.

After collection, each blood sample was immediately separated by centrifugation at 3000 rpm for 10 min. Then curcumin in the resulting samples was extracted twice with acetic ether from plasma. The mixture was vortexed for 3 min and centrifuged for 10 min at 3000 rpm. The supernatant was withdrawn and evaporated to remove the organic solvent under dry nitrogen atmosphere in water bath at 50 °C. The dry samples were re-dissolved in 100 μL methanol and centrifuged at 10,000 rpm for 10 min. 20 μL of supernatant was injected into HPLC system for determining curcumin in plasma samples.

2.7.2. In vivo antitumor efficacy studies

2.7.2.1. Animals and the establishment of tumor xenograft. Male athymic mice (BALB/c-nude mice, Nu/Nu strain), 4–6 weeks old, weighing 18–22 g were purchased from SLRC Laboratory Animal Ltd., Shanghai, China and were housed under controlled laboratory conditions in polycarbonate cages having free access to sterilized rodent pellet diet and acidified drinking water. All procedures were performed under sterile conditions in a laminar flow hood. This animal experiment was approved by the Institutional Animal Care and Use Committee and was in compliance with all regulatory guidelines.

Approximately, one million HepG2 cells, suspended in 200 μL of serum free medium were injected subcutaneously into one side of mice. Palpable solid tumors developed within 7–10 days post

tumor cell inoculation and once tumor masses became established (as soon as tumor volume reached ~125 mm^3), the animals were then randomized to receive either physiological saline, empty PBCA nanoparticles in aqueous solution (at a dose of 290 mg/kg) and curcumin-PBCA nanoparticles in aqueous solution (at a dose of 190 mg/kg) in 100 μL volumes for 4 weeks via intravenous injection (3 times weekly).

2.7.2.2. Evaluation of tumor growth suppression. Tumor size and body weight were measured with calipers once a week. The tumor volume was calculated using the following formula: volume = (length × $width^2$)/2, in which width was the shortest measurement in millimeters. Growth curves for groups of tumors are presented as the mean volume relative to the values on the first day of the treatment. At the end of the experiments, the animals were sacrificed by cervical dislocation and xenograft tumor tissues were harvested and preserved in 10% formalin solution for immunohistochemical studies.

2.8. Evaluation of in vivo VEGF and COX-2 levels in tumor tissues

We studied VEGF and COX-2 expression in the tumor tissue by immunohistochemical staining. Immunohistochemistry studies were performed by using formalin-fixed, paraffin embedded sections. Immunohistochemical analysis was carried out with the avidin-biotin complex immunoperoxidase technique as described previously (Allemann et al., 1993). Tumor sections were deparaffinaged in xylene. After blocking endogenous peroxidase and nonspecific antibody binding, rabbit polyclonal anti-COX-2 antibody or rabbit polyclonal anti-VEGF antibody was diluted at a ratio of 1:200 in 1% bovine albumin-containing PBS and the tumor sections were incubated for 1 h at room temperature. Staining was performed using avidin-biotin reagents, 3,3′-diaminobenzidine, and hydrogen peroxide. A secondary biotinylated antimouse antibody was added, followed by diaminobenzidine as a chromogen. The sections were lightly counterstained with hematoxylin and examined under light microscopy at ×200 magnifications.

2.9. Western blot analysis

Immunoblotting using standard procedures was performed to assess steady-state levels of COX-2 and VEGF protein.

Cells were washed with phosphate buffered saline and resuspended in ice-cold EBC buffer (0.5% Nonidet P-40, 50 mM Tris, pH 7.6, 120 mM NaCl, 1 mM EDTA, and 1 mM β-mercaptoethanol) with protease inhibitor mixture and lysed by sonication. The lysates were cleared of insoluble material by centrifugation at 14,000 rpm for 10 min at 4 °C. The supernatant was collected and aliquot into sterile microcentrifuge tubes, kept at −80 °C until it was used. A protein assay to measure protein content was performed by using the bicihonimic acid protein assay kit.

Samples containing 100 μg of protein were added into 4–14% SDS-PAGE. Aliquots of protein corresponding to 100 μg was mixed with SDS-PAGE sample buffer and heated on hot water bath for 5 min. The samples were resolved on a SDS-PAGE. The proteins were transferred on blotting grade nitrocellulose membrane. The membrane was treated with 5% non-fat dry milk and 0.1% PBS-Tween 20(milk-PBST) for 2 h at room temperature in order to block the non-specific sites on the membrane. Blots were probed with primary antibodies in anti-COX-2 antibody (1:200) and anti-VEGF antibody (1:200) for overnight at 4 °C. The membrane was then washed in 1× PBST three times for 5 min each followed by incubation with secondary antibody horseradish peroxidase conjugated donkey anti-rabbit IgG (1:5000) for 1 h at room temperature. The membrane was washed in 1× PBST four times for 10 min each; visualization of hybridization was carried out using chemiluminescence's reagent. The blots were exposed to autoradiography films 12.7 × 17.8 cm (Kodak X-OMAT BT) and developed.

2.10. Statistical analysis

Each experiment was conducted in triplicate and values were expressed as the mean SD. Comparison between the difference of means was performed by one-way ANOVA with the Tukey test applied post hoc for paired comparisons (SPSS 17.0) where p values of 0.05 or less were considered significant.

3. Results and discussion

3.1. Effect on particle size, surface properties and encapsulation efficiency

Particle size is an important parameter for drug delivery carriers. It has been suggested that particles smaller than 1 μm can undergo capillary distribution and uniform perfusion at the desired target site (Arias et al., 2001). Most solid tumors have elevated levels of vascular permeability. Particles less than 400 nm can cross vascular endothelia and accumulate at the tumor site via the EPR effect (Maeda et al., 2000; Monsky et al., 1999; Nomura et al., 1998).

The mean particle size for this type of nanoparticles as determined by dynamic light scattering was found to be about 200 nm with a narrow size distribution (Fig. 1(A)). TEM also show that the nanoparticles are spherical and well-separated, and most of them are smaller than 250 nm (Fig. 1(B)).

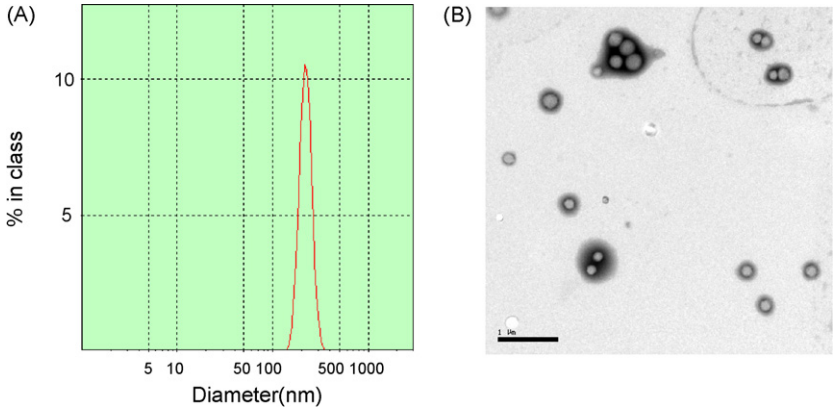

Fig. 1. The size distribution with dynamic light scattering (A) and the transmission electron microscopy (B) show that the curcumin-PBCA nanoparticles are completely spherical and an average diameter of <250 nm.

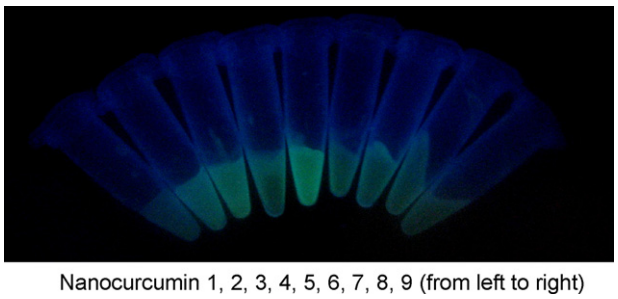

Fig. 2. Fluorescent images of the prepared curcumin-PBCA nanoparticles according to 3^2 factorial methods. 1–9 from left to right represent nanocurcumin 1 to nanocurcumin 9 respectively.

The surface charge of the nanoparticles is of interest since it influences the stability of the nanoparticle suspension and interactions of the nanoparticles with cell membrane. From zeta potential analysis, the empty PBCA nanoparticles have a little positive charge of 1.46 ± 0.03 mV on the surface. While the curcumin-PBCA nanoparticles have strong positive charge, even arrived at 29.11 ± 1.69 mV. The amounts of BCA monomer and stability chitosan have an effect on the zeta potential and encapsulation efficiency of curcumin-PBCA nanoparticles. The optimization batch 100 μL BCA and 10 mg chitosan to prepare curcumin-PBCA nanoparticles, that is the nanocurcumin 5 in Table 1. Its zeta potential and encapsulation efficiency are higher than others (data not shown). While the encapsulation efficiency is also be tested with the fluorescent images (Fig. 2) of different batches of curcumin-PBCA nanoparticles. The fluorescent intensity of nanocurcumin 5 is the strongest, which is coincidence with the highest encapsulation efficiency. It is reported that the higher zeta potential, the higher encapsulation efficiency (Zhang et al., 1994). This result is the same as the optimization batch in our experimental design.

While positively charged nanoparticles may have improved stability in the presence of biological cations and may be favorable for some drugs due to their interaction with negatively charged biological membranes and site-specific targeting *in vivo*. Chitosan has been used in the preparation and stabilization of polyester nanocapsules. It has been reported that polymerization of alkyl cyanoacrylates might occur via an anionic mechanism, a zwitterionic mechanism or both of them (Vauthier et al., 2003; Graf et al., 2009). Chitosan-containing amino and hydroxyl groups might act as nucleophilic agents to initiate the butyl cyanoacrylate monomer and is therefore present in the final polymer as end group according to the zwitterionic mechanism, resulting in characteristic change of this PBCA nanoparticle.

A series of curcumin-PBCA nanoparticles formulated with different amounts of curcumin in the ethanol phase were prepared to study the curcumin encapsulation efficiency. The encapsulation efficacy of curcumin in curcumin-PBCA nanoparticles is more than 60% when less than 0.02% (w/v) of curcumin was added to the solution (data not shown). An encapsulation efficiency of 90.4% can be achieved when the drug content is 0.01% (w/w) in the solution.

3.2. Cell culture assay

3.2.1. Curcumin-PBCA nanoparticles inhibits proliferation/survival of human hepatocellular carcinoma cell lines in vitro

We performed a series of *in vitro* functional assays to better characterize the anti-cancer properties of curcumin-PBCA nanoparticles, using human hepatocarcinoma cancer cells as a model system, and directly comparing its efficacy to free curcumin. Exposure to free and curcumin nanoparticles inhibited proliferation of tumor cells HepG2, Bel7402 and Huh7 cancer cells growth tested in a concentration and time-dependent manner (Fig. 3). Proliferation/survival was assessed by MTT assay.

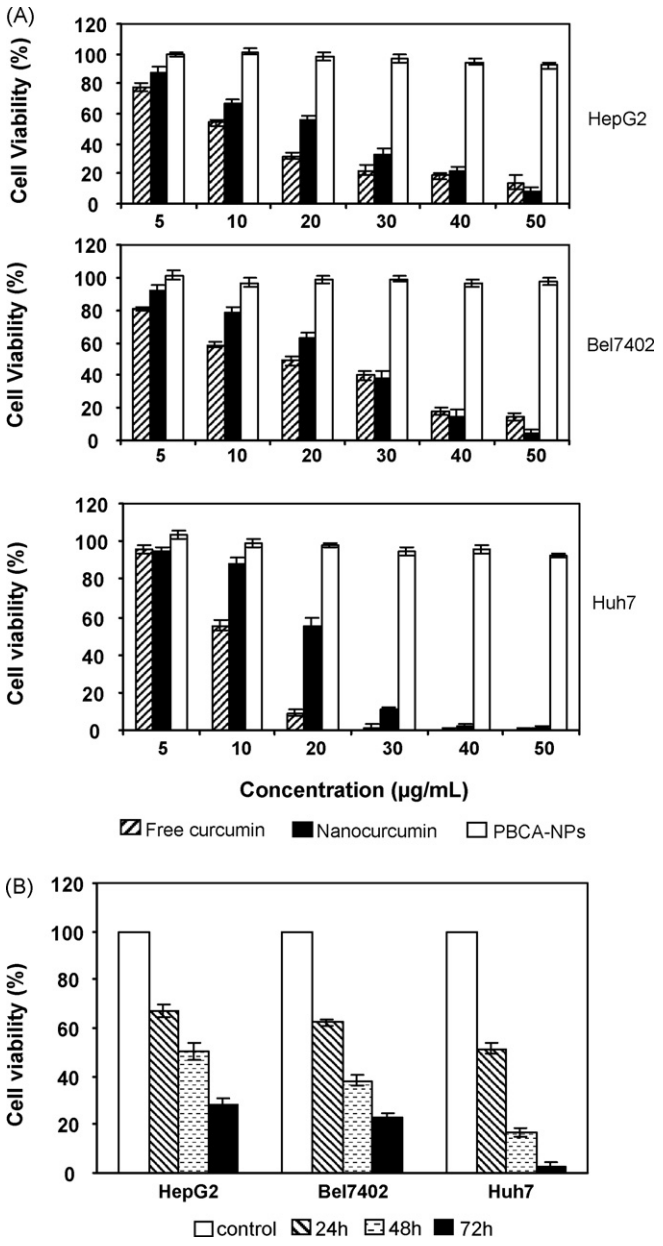

Fig. 3. Cytotoxicity of free curcumin and curcumin-PBCA nanoparticles against HepG2, Bel7402 and Huh7 cells. Data are presented as mean ± SD ($n = 6$). (A) Dose-dependent inhibition. (B) Time-dependent inhibition.

The results in Fig. 3(A) show that curcumin-PBCA nanoparticles suppressed cell proliferation dose-dependently at least as potently as native curcumin. The MTT assay shows that the viability of the cells incubated with empty PBCA nanoparticles remained at about 90% relative to the non-toxic control during the period of incubation (Fig. 3(A)). This indicates that within a concentration of 1 mg/mL empty PBCA nanoparticles imparts low cytotoxic effects to cells (Duan et al., 2009).

The effects of increasing curcumin-PBCA nanoparticles concentration in the medium from 5 to 50 μg/mL on the HepG2, Bel7402 and Huh7 cell viability are also shown in Fig. 3(A). The cell via-

bility decreases from 87.35% to 8.5%, 92.47% to 4.84% and 94.57% to 0.99%, respectively, as the curcurmin nanoparticles concentration increases from 5 to 50 μg/mL after 24 h incubation at 37 °C. The cytotoxic activity of curcumin-PBCA nanoparticles was also compared with that of free curcumin. Both free and curcumin nanoparticles inhibited the growth of human hepatocarcinoma cells. The results of cytotoxicity assay for free and encapsulated curcumin against HepG2 cells is shown in Fig. 3(A). After 24 h incubation with free curcumin at 5, 10, 20, 30, 40 and 50 μg/mL concentration, 77.32%, 53.9%, 32%, 22.36%, 18.98% and 14.01% of cells remained viable, respectively, while after cell treatment with curcumin nanoparticles at identical conditions 87.35%, 66.89%, 56.55%, 33%, 22.21% and 8.5% of cells remained viable, respectively. Similar results were observed in Bel7402 and Huh7 cells. After 24 h incubation, a significant difference in cell viability between free and polymeric encapsulated drug was observed at low and high curcumin concentration. Curcumin-PBCA nanoparticles demonstrated different cytotoxicity profile in comparison to free curcumin in different HCC cells under the study. In Bel7402 cells, polymeric curcumin nanoparticles were shown to be more effective than free curcumin at high concentrations (30, 40 and 50 μg/mL). While in HepG2 cells, curcumin nanoparticles were equally effective or less than free curcumin except at 50 μg/mL. In Huh7 cells, however, curcumin nanoparticles were always less effective than free curcumin at all tested concentrations.

Fig. 3(B) showed that after exposure to curcumin-PBCA nanoparticles for 24, 48 and 72 h, HepG2, Bel7402 and Huh7 cells were efficiently inhibited by curcumin nanoparticles (The concentrations of nanocurcumin were approximately 15 μg/mL for each cell line).

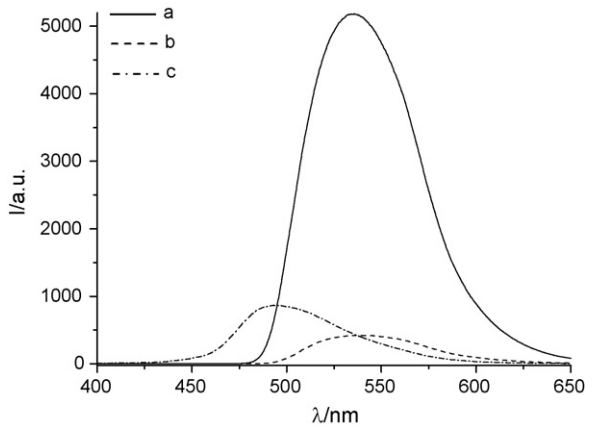

Fig. 4. Fluorescence emission spectra of curcumin in different solutions when excited at 285 nm. (a) Ethanolic solution of curcumin; (b) Curcumin in aqueous solution and ethanol (1:1, v/v); (c) Curcumin-PBCA nanoparticles in aqueous solution.

3.2.2. Cell uptake of curcumin-PBCA nanoparticles

The curcumin-PBCA nanoparticles show distinct photophysical properties (Fig. 4). Curcumin in aqueous solution and ethanol (1:1, v/v)(ethanol solution was used to solubilize curcumin, which was insoluble in pure water) has a broad fluorescent peak at 550 nm, the same wavelength as curcumin in absolute ethanol, whereas the curcumin-PBCA nanoparticles shows a well-defined blue-shifted fluorescent peak at 500 nm.

Taking advantage of the intrinsic green fluorescence of curcumin, we studied its cellular uptake by fluorescent microscopy.

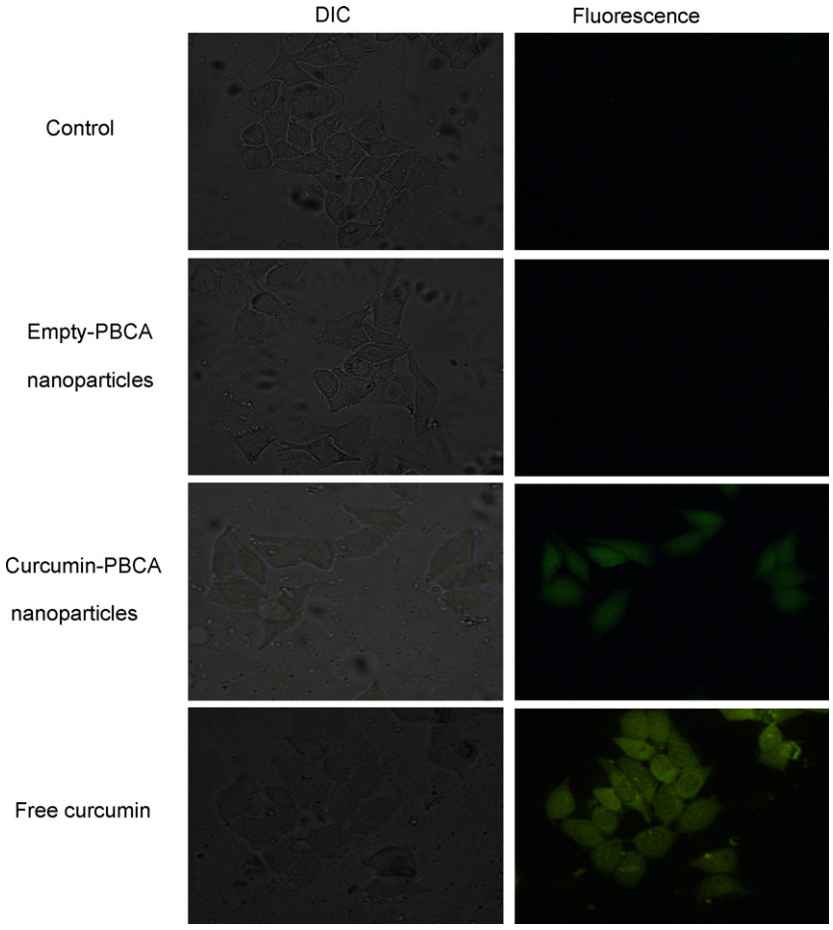

Fig. 5. Differential interference contrast (DIC) and fluorescence images of internalization of free and PBCA-loaded curcumin by HepG2 cells.

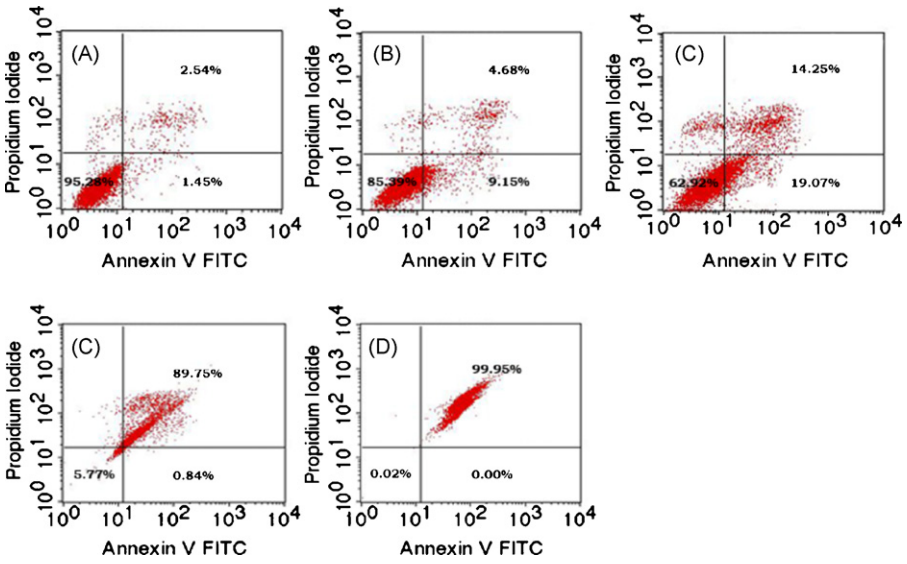

Fig. 6. Apoptotic cells detected by flow cytometry with annexin V conjugated with PI staining. HepG2 cells were treated with curcumin-PBCA nanoparticles at (A) control; (B) 10 μg/mL; (C) 20 μg/mL; (D) 40 μg/mL and (E) 60 μg/mL for 24 h.

Fig. 5 displays the microscopic images of fluorescence study. The microscopic images of control cells without any drug exposure and cells incubated with empty PBCA nanoparticles did not show any fluorescence, whereas the images of cells treated with encapsulated and free curcumin exhibited green fluorescence due to the internalized curcumin. So, cells can internalize polymeric encapsulated curcumin as effectively as free curcumin. However, the cationic curcumin-PBCA nanoparticles have the added advantage of enhanced solubility and can therefore be used directly without any organic solvent.

3.2.3. *Curcumin-PBCA nanoparticles induce apoptosis in HepG2 cell lines*

Consistent with the MTT assay, FACS analysis revealed a dose-dependent increase in the proportion of apoptotic cells in curcumin-PBCA nanoparticles treatments (Fig. 6).

Apoptosis was assessed by annexin V/PI staining (FACS analysis) after 24 h of exposure to curcumin nanoparticles. Annexin V binds to cells that express phosphatidylserine on the outer layer of the cell membrane, a characteristic feature of cells entering apoptosis. This allows discrimination of live cells (unstained by either fluorochrome) from apoptotic cells (stained with annexin V). Flow-cytometric analysis with annexin V/PI staining showed that when cells were exposed to curcumin nanoparticles for 24 h, the proportion of AV^+/PI^+ (necrotic cells) was increased from 2.54% of control cells to 14.25% of the 20 μg/mL curcumin group, and the number of AV^+/PI^- (apoptotic cells) increased from 1.45% to 19.07% (Fig. 6(C)). After 24 h treatment, the proportion of necrotic cells was increased from 2.54% of control cells to 89.75% of the 40 μg/mL curcumin group, and the number of AV^-/PI^- (viable cells) decreased from 95.28% to 5.77% (Fig. 6(D)) after treatment with 40 μg/mL curcumin nanoparticles. These results suggest that both necrosis and apoptosis contribute to the curcumin-induced death of HepG2 cells.

3.2.4. *Curcumin-PBCA nanoparticles inhibit expression of COX-2 and VEGF in vitro*

VEGF is known to be a specific stimulator of endothelial cell proliferation in many human cancers, and it is the most potent angiogenic factor regulating angiogenesis in HCC. Recent studies have highlighted the potential role of COX-2 in angiogenesis. COX-2 is involved in the regulation of VEGF-induced angiogenesis in HCC (Cheng et al., 2004). Overexpression of COX-2 has been demonstrated in HCC and HCC cell lines (Cervello and Montalto, 2006; Zhao et al., 2007). Moreover, a correlation between COX-2 expression and tumor angiogenesis in HCC has been identified in previous studies. These results indicated that targeting COX-2 to prevent HCC development might be a fascinating therapeutic strategy.

Curcumin has been shown to inhibit several angiogenic biomarkers including, VEGF and COX-2 expression (Aggarwal et al., 2005; Arbiser et al., 1998). The up-regulations of COX-2 protein expression in HepG2 groups were suppressed by treatment of curcumin-PBCA nanoparticles with a dose dependent manner. COX-2 has been implicated in the growth of tumors and steady state levels of COX-2 protein were assessed by Western blotting of protein extracts (100 μg per lane) derived from HepG2 Cell lines, both before and after exposure to different levels of free curcumin and curcumin nanoparticles for 48 hours. In COX-2 expressing lines, a dose-dependent decrease in COX-2 expression. Moreover, Fig. 7 also showed that the VEGF inhibition effects of curcumin nanoparticles were dose dependent manner as well. For both VEGF and COX-2, the suppressive effect of curcumin nanoparticles was equal to or greater than that of free curcumin at equimolar concentrations. Therefore, curcumin could be used as a candidate for the combined drug treatment for HCC in the future.

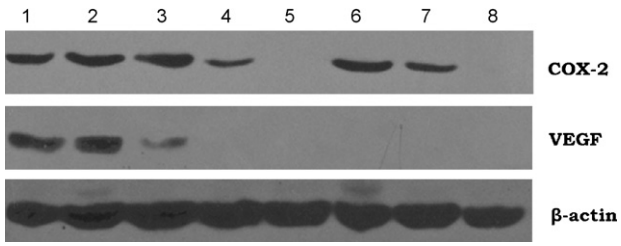

Fig. 7. Effect of curcumin-PBCA nanoparticles on cyclooxygenase-2 and vascular endothelial growth factor as assessed by western blot analysis. Lane 1: control; lane 2: empty PBCA nanoparticles; lane 3–5: correspond to 5 μg/mL, 15 μg/mL and 30 μg/mL of free curcumin, respectively; lane 6–8: represent 5 μg/mL, 15 μg/mL, and 30 μg/mL of curcumin-PBCA nanoparticles.

Table 2
The pharmacokinetic parameters of free curcumin (10 mg/kg, i.v.) and curcumin-PBCA nanoparticles (5 mg/kg, i.v.) in rats ($n = 3$).

Pharmacokinetic parameters	Free curcumin	Curcumin-PBCA nanoparticles
$AUC_{0-\infty}$ (mg/L h)	1.922	3.302
$t_{1/2\beta}$ (h)	0.362	18.661
$MRT_{0-\infty}$ (h)	0.159	63.787
CL (L/h/kg)	0.005	0.002
V_d (L/kg)	0.002	0.103

3.3. In-vivo study of curcumin-PBCA nanoparticles

3.3.1. Pharmacokinetic parameters

The data for pharmacokinetics in mice were analyzed with DAS 2.1.1(SHUTCM shanghai, China), and pharmacokinetic parameters were shown in Table 2. The pharmacokinetic behavior in mice by i.v. administration of free curcumin and curcumin-PBCA nanoparticles followed two-compartment model. Encapsulation of curcumin in the PBCA nanoparticles caused a profound change in the pharmacokinetics of the drug. The elimination half-life of curcumin was increased 52-fold when it was in the complex form with PBCA nanoparticles and eventually the clearance of the molecule in complex form was also 2.5-fold decreased. A decreased CL is expected if the circulating drug is sufficiently restricted to the blood compartment as a result of being confined within circulating micelles. The area under the curve ($AUC_{0-\infty}$) after i.v. injection of curcumin-PBCA nanoparticles was 3.302 mg/L h, while 1.922 mg/L h for $AUC_{0-\infty}$ of free curcumin despite a 2-fold dose being administered compared with nanoparticles formulation.

The higher plasma concentration of curcumin for curcumin-PBCA nanoparticles might be a result of the size of nanoparticles and chitosan coating on the surface to keep the formulation in the circulation for an extended period.

Besides, the mean residence time ($MRT_{0-\infty}$) of curcumin-PBCA nanoparticles (63.787 h) was longer than that of free curcumin (0.159 h). These results might be due to accumulation of nanoparticles in RES organs and sustained release of drug from those tissues. Moreover, the properties of particles (such as shape, size, charge, and hydrophilicity) can prolong the retention of them in the blood compartment.

There was a substantial increase in the volume of distribution (51-fold). The increase in V_d was quite unexpected, however. It was possible that the larger micellar particles, formed after concentrating micellar population, were sequestered by the reticuloendothelial system or other tissues, which released the encapsulated drug as a reservoir, and led to the greatly increased V_d (Kommareddy et al., 2005).

3.3.2. Curcumin-PBCA nanoparticles inhibit the growth of hepatocarcinoma tumor xenografts

Curcumin-PBCA nanoparticles were also active *in vivo* models. As depicted in Fig. 8(A) and (C), treatment with curcumin nanoparticles resulted in significant growth retardation of HepG2 xenograft tumors compared with control or empty PBCA nanoparticles-treated mice. The results of tumor volume changes as a function of time with curcumin-PBCA nanoparticles are shown in Fig. 8(C). In HepG2 models, the average tumor volumes at day 24 after initiation of therapy were as follows: 936 mm^3 for physiological saline, 864 mm^3 for empty PBCA nanoparticles in aqueous solution, 407.5 mm^3 for curcumin-PBCA nanoparticles in aqueous solution. Curcumin nanoparticles had significant growth suppressive effects compared with control vehicles (saline or empty PBCA nanoparticles). No behavioral abnormalities or weight loss was observed during the course of therapy in any of the mice receiving empty PBCA nanoparticles (Fig. 8(B)).

Because poly(alkyl)cyanoacrylates (PACAs) are biocompatible and biodegradable, butylcyanoacrylate has received FDA approval for human use (Graf et al., 2009). Degradation products consist of an alkylalcohol and poly(cyanoacrylic acid), which are soluble in water and be eliminated *in vivo* via kidney filtration (Zhang et al., 1994).

Treatment with curcumin nanoparticles resulted in reduced tumor size and visible blanching of tumors (Fig. 8). In addition,

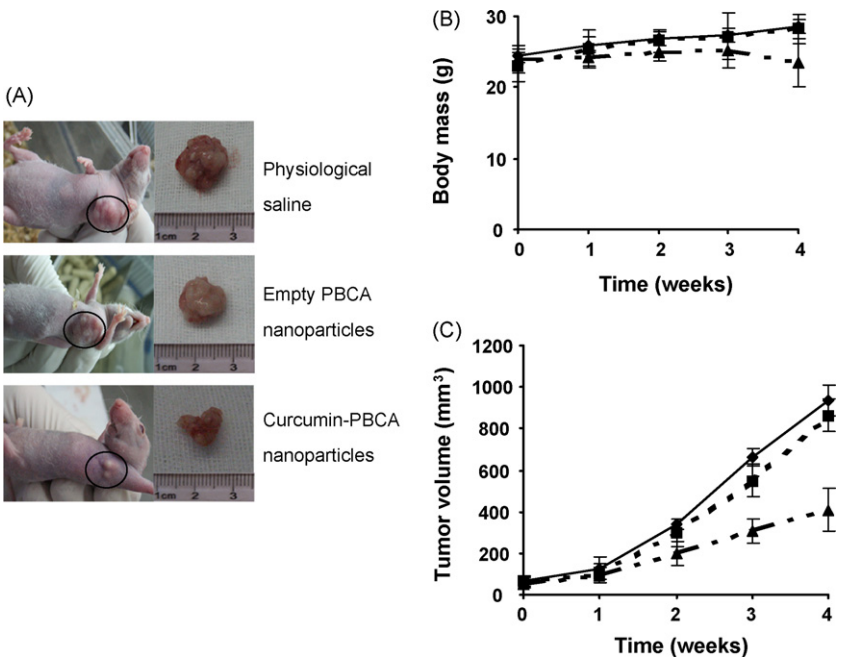

Fig. 8. *In vivo* efficacy of curcumin-PBCA nanoparticles and empty PBCA nanoparticles in HepG2 hepatocellular cancer xenograft. (A) The images of HepG2 xenograft-bearing mice treated with curcumin-PBCA nanoparticles, empty PBCA nanoparticles and control tumor; changes in body weight of animals (B) and tumor volume (C) as a function of time in subcutaneous HepG2 xenograft. Straight line: physiological saline; dashed line: empty PBCA nanoparticles; double dot dashed line: curcumin PBCA nanoparticles.

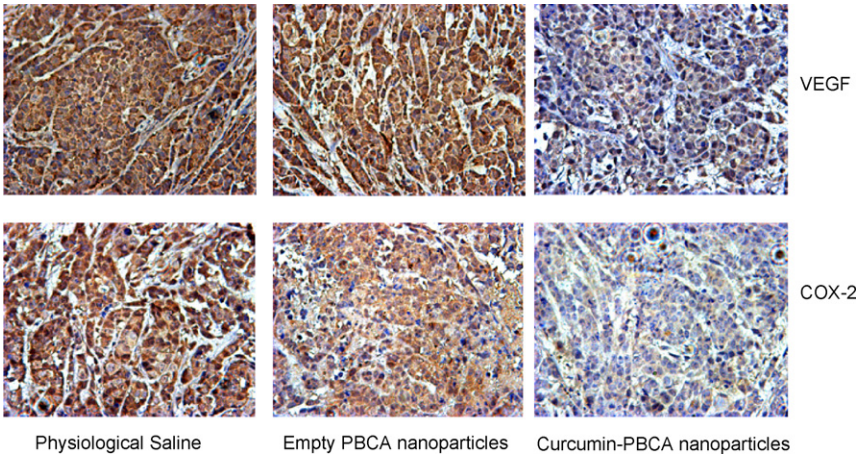

Fig. 9. Antiangiogenic effect of curcumin-PBCA nanoparticles *in vivo*. Immunohistochemistry of tumor sections using anti-VEGF and anti-COX-2.

expression of VEGF, as well as COX-2, was decreased in HepG2 tumor xenografts (by immunohistochemistry analysis), consistent with an antiangiogenic effect (Fig. 9).

4. Conclusions

This malignancy is highly resistant to chemotherapy. The bioavailability of curcumin is, however, poor. The prepared chitosan stabilized PBCA nanoparticles can entrap the curcumin effectively and circumvent this problem by permitting intravenous administration. The results presented in the current study demonstrate that curcumin nanoparticles and free curcumin are both to suppress COX-2 and VEGF expression, as well as cell proliferation/survival of hepatocarcinoma carcinoma cells. *In vivo*, curcumin nanoparticles inhibit hepatocarcinoma cell growth in murine xenograft models and these effects are accompanied by a potent antiangiogenic response. Curcumin possesses both direct and indirect anti-angiogenic activity both *in vitro* and *in vivo*. Therefore, curcumin-PBCA nanoparticles provide an opportunity to expand the clinical repertoire of this efficacious agent by enabling ready aqueous dispersion.

Acknowledgements

This study was supported by the State 863 Program in the Eleventh Five-Year Plan (No. 2007AA021809) and the Graduate degree thesis Innovation Foundation of Central South University (No.CX2009B052). Transmission electron microscopy was performed by Professor Zhu xiaojing at the Electron Microscopy Center of Central South University.

References

Aggarwal, B.B., Harikumar, K.B., 2009. Potential therapeutic effects of curcumin, the anti-inflammatory agent, against neurodegenerative, cardiovascular, pulmonary, metabolic, autoimmune and neoplastic diseases. Int. J. Biochem. Cell Biol. 1, 40–59.

Aggarwal, B.B., Kumar, A., Bharti, A.C., 2003. Anticancer potential of curcumin: preclinical and clinical studies. Anticancer Res. 23, 363–398.

Aggarwal, B.B., Shishodia, S., Takada, Y., Banerjee, S., Newman, R.A., Bueso-Ramos, C.E., Price, J.E., 2005. Curcumin suppresses the paclitaxel-induced nuclear factor-kappaB pathway in breast cancer cells and inhibits lung metastasis of human breast cancer in nude mice. Clin. Cancer Res. 11, 7490–7498.

Allemann, E., Gurny, R., Doelker, E., 1993. Drug-loaded nanoparticles: preparation methods and drug targeting issues. Eur. J. Pharm. Biopharm. 39, 173–191.

Anand, P., Kunnumakkara, A.B., Newman, R.A., Aggarwal, B.B., 2007. Bioavailability of curcumin: problems and promises. Mol. Pharm. 4, 807–818.

Arbiser, J.L., Klauber, N., Rohan, R., Leeuwen, R.V., Huang, M.T., Fisher, C., Flynn, E., Byers, H.R., 1998. Curcumin is an *in vivo* inhibitor of angiogenesis. Mol. Med. 4, 376–383.

Arias, J.L., Gallardo, V., Gomez-Lopera, S.A., Plaza, R.C., Delgado, A.V., 2001. Synthesis and characterization of poly (ethyl-2-cyanoacrylate) nanoparticles with a magnetic core. J. Controlled Release 77, 309–321.

Behan, N., Birkinshaw, C., Clarke, N., 2001. Poly *n*-butyl cyanoacrylate nanoparticles: a mechanistic study of polymerization and particle formation. Biomaterials 22 (11), 1335–1344.

Belakavadi, M., Salimath, B.P., 2005. Mechanism of inhibition of ascites tumor growth in mice by curcumin is mediated by NF-kB and caspase activated Dnase. Mol. Cell. Biochem. 273, 57–67.

Bisht, S., Feldmann, G., Soni, S., Ravi, R., Karikar, C., Maitra, A., 2007. Polymeric nanoparticle-encapsulated curcumin (“nanocurcumin”): a novel strategy for human cancer therapy. J. Nanobiotechnol. 5, 1–18.

Cervello, M., Montalto, G., 2006. Cyclooxygenases in hepatocellular carcinoma. World J. Gastroenterol. 12, 5113–5121.

Cheng, A.L., Hsu, C.H., Lin, J.K., Hsu, M.M., Ho, Y.F., Shen, T.S., Ko, J.Y., Lin, J.T., Lin, B.R., Ming-Shiang, W., Yu, H.S., Jee, S.H., Chen, G.S., Chen, T.M., Chen, C.A., Lai, M.K., Pu, Y.S., Pan, M.H., Wang, Y.J., Tsai, C.C., Hsieh, C.Y., 2001. Phase I clinical trial of curcumin, a chemopreventive agent, in patients with high-risk or pre-malignant lesions. Anticancer Res. 21, 2895–2900.

Cheng, A.S., Chan, H.L., To, K.F., Leung, W.K., Chan, K.K., Liew, C.T., 2004. Cyclooxygenase-2 pathway correlates with vascular endothelial growth factor expression and tumor angiogenesis in hepatitis B virus-associated hepatocellular carcinoma. Int. J. Oncol. 24, 853–860.

Couvreur, P., Vauthier, C., 1991. Polyalkylcyanoacrylate nanoparticles as drug carrier: present state and perspectives. J. Controlled Release 17, 187–198.

Dai, W.Q., Zhou, C.J., Cui, L.L., Ren, H.B., Zhao, W.Q., 2004. The advance in research on drug-loaded nanoparticle of polybutylcyanoacrylate. Pharm. Care Res. 4 (1), 33–35.

Douglas, S.J., Illum, L., Davis, S.S., Kreuter, J., 1984. Particle size and size distribution of poly(butyl-2-cyanoacrylate) nanoparticles I: Influence of physicochemical factors. J. Colloid Interface Sci. 101, 149–158.

Douglas, S.J., Illum, L., Davis, S.S., 1985. Particle size and size distribution of poly(butyl 2-cyanoacrylate) nanoparticles II: Influence of stabilizers. J Colloid Interface Sci. 103, 154–163.

Duan, J.H., Zhang, Y.D., Chen, W., Shen, C.R., Liao, M.M., Pan, Y.F., Wang, J.W., Deng, X.M., Zhao, J.F., 2009. Cationic polybutyl cyanoacrylate nanoparticles for DNA delivery. J. Biomed. Biotechnol. 2009, 1–9.

Goel, A., Kunnumakkara, A.B., Aggarwal, B.B., 2008. Curcumin as “Curecumin”: from kitchen to clinic Biochem. Pharmacology 75, 787–809.

Graf, A., McDowell, A., Rades, T., 2009. Poly(alkycyanoacrylate) nanoparticles for enhanced delivery of therapeutics—is there real potential? Expert Opin. Drug Deliv. 6 (4), 371–387.

Gururaj, A.E., Belakavadi, M., Venkatesh, D.A., Marme, D., Salimath, B.P., 2002. Molecular mechanisms of anti-angiogenic effect of curcumin. Biochem. Biophys. Res. Commun. 297, 934–942.

Huang, C.Y., Chen, C.M., Lee, Y.D., 2007. Synthesis of high loading and encapsulation efficient paclitaxel-loaded poly(n-butyl cyanoacrylate) nanoparticles via miniemulsion. Int. J. Pharm. 338, 267–275.

Juan, B.S.D., Briesen, H.V., Gelperima, S.E., Kreuter, J., 2006. Cytotoxicity of doxorubicin bound to poly(butyl cyanoacrylate) nanoparticles in rat glioma cell lines using different assays. J. Drug Target. 14 (9), 614–622.

Kommareddy, S., Tiwari, S.B., Amiji, M.M., 2005. Long-circulating polymeric nanovectors for tumor-selective gene delivery. Technol. Cancer Res. Treat. 4, 615.

Kunwar, A., Barik, A., Pandey, R., Priyadarsini, K.I., 2006. Transport of liposomal and albumin loaded curcumin to living cells: an absorption and fluorescence spectroscopic study. Biochim. Biophys. Acta 1760, 1513–1520.

Lescure, F., Zimmer, C., Roy, D., Couvreur, P., 1992. Optimization of polyalkylcyanoacrylate nanoparticle preparation: influence of sulfur dioxide and pH on nanoparticle characteristics. J. Colloid Interface Sci. 154, 77–86.

Maeda, H., Wu, J., Sawa, T., Matsumura, Y., Hori, K., 2000. Tumor vascular permeability and the EPR effect in macromolecular therapeutics: a review. J. Controlled Release 65, 271–284.

Maiti, K., Mukherjee, K., Gantait, A., Saha, B.P., Mukherjee, P.K., 2007. Curcumin-phospholipid complex: preparation, therapeutic evaluation and pharmacokinetic study in rats. Int. J. Pharm. 330, 155–163.

Maksimenko, O., Pavlov, E., Toushov, E., Molin, A., Stukalov, Y., Prudskova, T., Feldman, V., Kreuter, J., Gelperina, S., 2008. Radiation sterilization of doxorubicin bound to poly(butyl cyanoacrylate) nanoparticles. Int. J. Pharm. 356 (1–2), 325–332.

Marczylo, T.H., Verschoyle, R.D., Cooke, D.N., Morazzoni, P., Steward, W.P., Gescher, A.J., 2007. Comparison of systemic availability of curcumin with that of curcumin formulated with phosphatidylcholine. Cancer Chem. Pharmacol. 60, 171–177.

Miyazaki, S., Takahashi, A., Kubo, W., 2003. Poly n-butylcyanoacrylate (PNBCA) nanocapsules as a carrier for NSAIDs: *in vitro* release and *in vivo* skin penetration. J. Pharm. Pharm. Sci. 6, 240–245.

Monsky, W.L., Fukumura, D., Gohongi, T., Ancukiewcz, M., Weich, H.A., Torchilin, V.P., Yuan, F., Jain, R.K., 1999. Augmentation of transvascular transport of macromolecules and nanoparticles in tumors using vascular endothelial growth factor. Cancer Res. 59, 4129–4135.

Nomura, T., Koreeda, N., Yamashita, F., Takakura, Y., Hashida, M., 1998. Effect of particle size and charge on the disposition of lipid carriers after intratumoral injection into tissue-isolated tumors. Pharm. Res. 15, 128–132.

Page-Clisson, M.E., Pinto-Alphandary, H., Ourevitch, M., Andremont, A., Couvreur, P., 1998. Development of ciprofloxacin-loaded nanoparticles: physicochemical study of the drug carrier. J. Controlled Release 56, 23–32.

Petri, B., Bootz, A., Khalansky, A., Hekmatara, T., Müller, R., Uhl, R., Kreuter, J., Gelperina, S., 2007. Chemotherapy of brain tumour using doxorubicin bound to surfactant-coated poly(butyl cyanoacrylate) nanoparticles: revisiting the role of surfactants. J. Controlled Release 117, 51–58.

Reddy, L.H., Sharma, R.K., Murthy, R.S.R., 2004. Enhanced tumour uptake of doxorubicin loaded poly(butyl cyanoacrylate) nanoparticles in mice bearing Dalton's lymphoma tumour. J. Drug Target. 12 (7), 443–451.

Salmaso, S., Bersani, S., Semenzato, A., Caliceti, P., 2007. New cyclodextrin bioconjugates for active tumor targeting. J. Drug Target. 15, 379–390.

Shishodia, S., Amin, H.M., Lai, R., Aggarwal, B.B., 2005. Curcumin (diferuloylmethane) inhibits constitutive NF-kappaB activation, induces G1/S arrest, suppresses proliferation, and induces apoptosis in mantle cell lymphoma. Biochem. Pharmacol. 70, 700–713.

Shoba, G., Joy, D., Joseph, T., Majeed, M., Rajendran, R., Srinivas, P.S., 1998. Influence of piperine on the pharmacokinetics of curcumin in animals and human volunteers. Planta. Med. 64, 353–356.

Siwak, D.R., Shishodia, S., Aggarwal, B.B., Kurzrock, R., 2005. Curcumin-induced antiproliferative and proapoptotic effects in melanoma cells are associated with suppression of IkappaB kinase and nuclear factor kappaB activity and are independent of the B-Raf/mitogen-activated/extracellular signal-regulated protein kinase pathway and the Akt pathway. Cancer 104, 879–890.

Sou, K., Inenaga, S., Takeoka, S., Tsuchida, E., 2008. Loading of curcumin into macrophages using lipid-based nanoparticles. Int. J. Pharm. 352, 287–293.

Tasset, C., Barette, N., Thysman, S., Ketelslegers, J.M., Lemoine, D., Preat, V., 1995. Polyisobutylcyanoacrylate nanoparticles as sustained release system for calcitonin. J. Controlled Release 33, 23–30.

Tiyaboonchai, W., Tungpradit, W., Plianbangchang, P., 2007. Formulation and characterization of curcuminoids loaded solid lipid nanoparticles. Int. J. Pharm. 337, 299–306.

Tonnesen, H.H., Masson, M., Loftsson, T., 2002. Studies of curcumin and curcuminoids XXVII. Cyclodextrin complexation: solubility, chemical and photochemical stability. Int. J. Pharm. 244, 127–135.

Vauthier, C., Dubernet, C., Fattal, E., Pinto-Alphandary, H., Couvreur, P., 2003. Poly(alkylcyanoacrylates) as biodegradable materials for biomedical applications. Adv. Drug Deliv. Rev. 55, 519–548.

Vemula, P.K., Li, J., John, G., 2006. Enzyme catalysis: tool to make and break amygdalin hydrogelators from renewable resources: a delivery model for hydrophobic drugs. J. Am. Chem. Soc. 128, 8932–8938.

Wang, Y.J., Pan, M.H., Cheng, A.L., Lin, L.I., Ho, Y.S., Hsieh, C.Y., Lin, J.K., 1997. Stability of curcumin in buffer solutions and characterization of its degradation products. J. Pharm. Biomed. Anal. 15, 1867–1876.

Zhang, Z.R., Liao, G.T., Hou, S.X., 1994. Study on mitoxantrone polycyanoacrylate nanospheres. Acta Pharmacol. Sin. 29 (7), 544–549.

Zhao, Q.T., Yue, S.Q., Cui, Z., Wang, Q., Cui, X., Zhai, H.H., Zhang, L.H., Dou, K.F., 2007. Potential involvement of the cyclooxygenase-2 pathway in hepatocellular carcinoma-associated angiogenesis. Life Sciences 80, 484–492.

Zheng, M., Ekmekcioglu, S., Walch, E.T., Tang, C.H., Grimm, E.A., 2004. Inhibition of nuclear factor-kappaB and nitric oxide by curcumin induces G_2/M cell cycle arrest and apoptosis in human melanoma cells. Melanoma Res. 14, 165–171.